ICEM12- 12th International Conference on Experimental Mechanics
29 August - 2 September, 2004 Politecnico di Bari, Italy

CHECKUP FOR AGING ARTWORK: OPTICAL TOOLS TO MONITOR MECHANICAL BEHAVIOUR

K.D. Hinsch, G. Gülker, H. Helmers

Applied Optics, Institute of Physics, Carl von Ossietzky University Oldenburg, D-26111 Oldenburg, GERMANY, klaus.hinsch@uni-oldenburg.de

ABSTRACT

Deterioration of artwork is often connected to mechanical material degradation that starts on microscopic scales. Insight into decay mechanisms can therefore be obtained by monitoring microscopic deformation and displacement fields. Thus, the proper optical methods become an ideal tool for restorers and conservators, the more as they are non-intrusive and remotely applicable. We show how the scope of modern coherent metrology can be adapted to this aim. Refinements of correlation imaging, speckle interferometry and low-coherence detection provide a wealth of methods that have been applied successfully in historical objects.

1. INTRODUCTION

For many years the preservation of artwork was mainly the domain of the humanities. Lately, however, science is playing an increasing role in the analysis, conservation and restoration of historical objects. For such unique and delicate specimens, analytical techniques must be non-invasive. Optics is providing a powerful and versatile set of tools for surveying and analyzing historical treasures [1,2]. These priceless objects have aged since they were made. They deteriorate due to varying climate conditions or polluted environments and their preservation requires special countermeasures. Critical monitoring of the state of the object (comparable to the regular medical checkup in health care), identification and understanding of the deterioration processes and control of any remedies are important.

Often decay starts at the microscopic level initially producing weakening of the mechanical cohesion in the sample. This shows up in irregular minute displacements or changes in the micro-topography of the object’s surface. Thus, optical deformation mapping methods can provide essential data on the distribution of mechanical loads in the sample, indicate weak spots, or provide early warning data in objects at risk. Suitable methods must provide sufficient sensitivity to detect displacements or changes in the topography well in the micrometer domain and still operate successfully on-site in spite of disturbances like rigid-body creeping motions, annoying vibrations or air turbulence.

An early method of choice has been electronic speckle pattern interferometry (ESPI) that offers sub-wavelength sensitivity in a rigid and compact portable instrument [3]. The object under investigation is imaged under laser illumination by a CCD-camera such that the speckles are resolved. In the basic setup a suitably tailored reference wave is superimposed to produce an interference image (image plane hologram) available for further processing in a computer. Subtraction of successive images, e.g., yields so-called correlation fringes that represent lines of constant displacement in the direction of the sensitivity vector determined by illumination and observation geometry. Since the interpretation of fringe systems is difficult and even ambiguous, phase shifting strategies from ordinary interferometry were adapted. The recording of several images with well-defined phase shifts in the reference wave allows automated evaluation by spatial phase unwrapping and provides unambiguous deformation data [4].

This method is state-of-the-art today and has proven very powerful in monitoring displacement fields in many applications. In the study of artwork, however, the specific situation of a delicate object, and often an unfavorable measurement environment present challenges that inspired sophisticated refinements of some basic techniques and even novel approaches which will be the theme of this presentation.

2. HISTORICAL CASE STUDY: SUNSHINE ON FRESCOS

To introduce the matter, outline the problems that needed improvements and illustrate the type of data obtained we show some early results from a project where traditional ESPI provided answers to questions of the conservators. The study concerned the role of solar irradiation in the decay of 19th-century murals in *Wartburg* castle of *Thuringia*, Germany. This castle is the famous place where Martin Luther translated the bible into German around 1520. The legend says that he had to fend off the devil by throwing his inkpot at him! A conventional ESPI-system with laser-diode illumination and phase shifting by piezoelectric tilt of a glass plate in the reference wave was rigidly attached to the wall. The thermal load on the fresco was estimated by mapping deformations during cyclic heating and cooling. Fig. 1 shows at the left the area of observation in the mural and at the right the deformation field produced within a 2.5-minute period during a cooling-off phase. A characteristic feature is a sudden kink in the displacement running through the field and coinciding with an image detail in the painting. Obviously, such an abrupt change will be accompanied by high local tensions in the material that will pose a threat to the integrity of the substance – a good reason to ban all direct sunlight from the frescos. The coincidence with the feature line provided an interesting explanation for the discontinuity in the mechanical response. It is here that two pieces of work meet that the painter has produced at different times. Frescos are painted onto fresh plaster and the artist scrapes off unused plaster when he finishes a day’s work. The measurement suggests

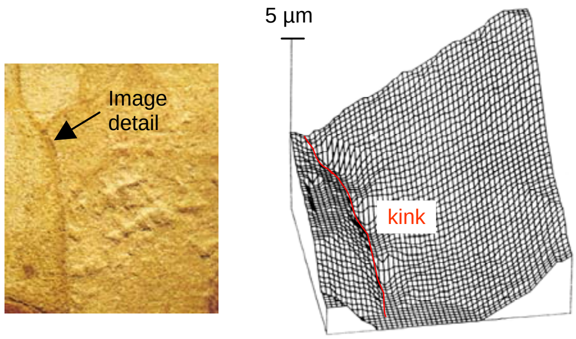

Fig.1. ESPI study of the thermal response of a fresco in *Wartburg* castle, *Thuringia*, Germany. Left: measuring field (width 6 cm); right: displacement map showing deformation kink at location of former boundary of work-piece.

that new plaster does not attach well to the old. The reduced mechanical contact is a source for future problems. Thus, 150 years after the frescos were painted we uncovered where the artist made a break in his work – although he tried to hide it underneath a feature line in the image!

This example is typical for a specific feature of optical metrology in the monitoring of artwork. Long-term changes in a specimen are revealed in a regular checkup by repeatedly exposing a specimen to a standard load and studying any changes in its response. Since restorers and conservators who usually are not trained technically are to understand the results of complex metrology the acceptance of a method depends also on the proper presentation and visualization of data.

In the course of further activities it was realized that early-day ESPI needed substantial improvements to cope with the problems generally met in the practical study of artwork. It suffered from spurious signal fluctuations during observation and data acquisition that originated from background vibrations, turbulence in the optical path or rigid-body misalignments. Sometimes the technique was just too sensitive for the process encountered, sometimes the deformation rate was too rapid to obtain correct phase-shifted data; often the light source lacked coherence or was instable. We will now turn towards more refined techniques that take up such shortcomings and provide some new innovative approaches.

3. MODIFICATIONS OF ESPI

Any up-to-date operation of ESPI requires provisions for phase shifting. Several frames are needed for each state of the object that have been taken at a set of given phase differences between object and reference wave. We have seen that such phase shifts can be produced in succession by changing the optical path in one branch – termed temporal phase shifting TPS. Processing of the phase-shifted frames produces a phase map mod2π which is usually displayed in a saw tooth gray-level representation.

During live observations of non-stationary objects like pieces of art the conditions may change in time faster than allowed by the time-out required for phase shifting. Even if the object deformation is sufficiently slow, often the measured phase is deteriorated by air turbulences in the optical path or by background vibrations. Schemes have therefore been developed to obtain the phase data simultaneously.

The most successful concept in which at least three phase-shifted images are recorded on the same CCD-target is called spatial phase shifting SPS [5,6]. For this purpose the origin of the spherical reference wave in the aperture of the imaging optics is given a small lateral offset resulting in a linear increase of phase in the target. The offset can be adjusted such that the period of the resulting carrier fringes equals three times the pixel pitch in the offset direction. The reference phase between adjacent pixels therefore differs by 120° and the combination of data from three neighboring pixels gives the necessary phase-shifted frames. These can be combined in the commonly used phase-shifting algorithms to produce the mod2π saw tooth pattern. For our purposes another evaluation method, the Fourier-transform technique [7], is more appropriate, because it offers additional features as we will see subsequently.

Let us briefly recall this technique. The superposition of the object-light speckle pattern with an off-axis reference wave creates a modulation with a carrier fringe pattern. Fourier-transformation of the CCD-image thus produces a zero-order and two side-bands both of which contain the complex spatial frequency spectrum of the object light. Careful matching of pixel data (size and pitch), speckle size and reference wave offset will guarantee non-overlapping terms and maximum free spectral range. The possibility to subtract the speckle halo even relaxes the offset requirement. Any one of the sidebands can be separated for inverse Fourier-transformation to yield the complex object light distribution from which the wanted phase is obtained.

Let us demonstrate the superiority of SPS over TPS by observing a static deformation (point-like load at the center of a membrane) that is disturbed by background vibration (insufficient vibration insulation of the setup) or hot turbulent air in the viewing path (Fig. 2). Obviously, TPS results in poor-quality saw tooth images because vibrations cause wrong phase shifts and thus a loss of directional information, and small-scale turbulence creates even locally varying phase shifts so that the correctness of the image is partly lost. Due to the greatly improved performance of SPS we decided therefore to implement this arrangement whenever possible. Comparison of both the left images, however, illustrates that under static conditions SPS performs slightly inferior due to residual fluctuating speckle phase over the three pixels compared [8].

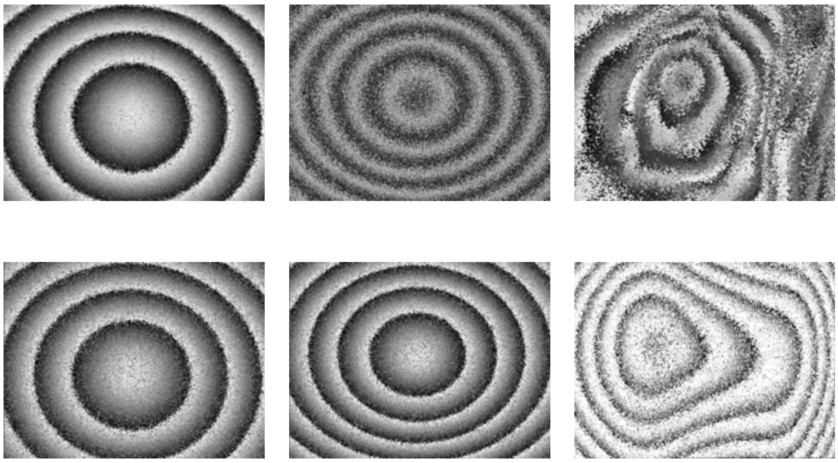

Fig. 2. Deterioration of the saw tooth phase maps in an ESPI deformation study under stable experimental conditions (left) and disturbed by vibrations (center) or air turbulence (right). Performance of temporal phase shifting TPS (above) versus spatial phase shifting SPS (below).

For an overall displacement map characterizing the process under investigation the steps in the mod2π-maps have to be eliminated – a procedure called spatial phase unwrapping. The usual way is to detect locations of the 2π jumps by comparing neighboring phase values and converting the step function into a continuous displacement phase by adding the required integer multiples of 2π. This procedure is carried out along suitable tracks in the image – thus the name spatial phase unwrapping. In the history of ESPI, effective unwrapping algorithms that are resistant to a propagation of errors have been an important issue. They easily work in good-quality data fields. Real-world objects like those we are concerned with in this article, however, pose real challenges.

The problem can be nicely illustrated by the response of a piece of historic brick, 2 cm in thickness, to cyclic heating and cooling with an infrared radiator (Fig. 3). The white-light image of the specimen in the left of Fig. 3 already implies some difficulties to expect. We see that a network of cracks divides the brick into numerous sub-areas that probably each will execute an independent deformation. Indeed, the out-of-plane displacement phase map mod2π in the center image reveals several areas of irregular boundaries that have undergone separate motion as indicated by the varying fringe densities and orientations.

For spatial unwrapping the areas would need identification and separate evaluation – quite a laborious task. Even more, the saw tooth image does not render any information as to the relative heights in the sub-areas because the absolute fringe order within each area is not known – we have no information about the fringe count during the period between capturing images. Yet, this is an important quantity in estimating the distribution of mechanical loads between sub-areas in the specimen.

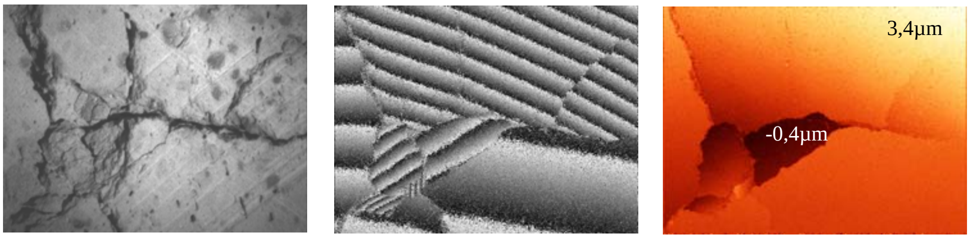

Fig. 3. Mapping of out-of-plane displacements in a historic brick specimen due to heat irradiation. Left: white-light image; center: mod2π phase map; right: displacement obtained by temporal phase unwrapping.

A solution to this problem is given by temporal phase unwrapping [9]. It makes use of the rapid data rate available in recent image acquisition and processing equipment. The phase history at every single pixel in the camera is stored – in combination with SPS we now get saw tooth data versus time. Since images are stored at a rate excluding intermediate phase changes of more than $\pm\pi$ no ambiguous phase jumps are encountered. Thus, we are not bothered by any irregularities in space and unwrapping even yields the relative displacements between the sub-areas. Let us prove this by looking at the result in the right of Fig. 3 where the amount of displacement – ranging from -0.4 µm to 3.4 µm – is encoded in color. In such cases, an important question by restorers is whether the deformation in the specimen is reversible and the object follows the cyclic load by cyclic motion. This could, of course, be answered only on the basis of absolute data as in Fig. 3 right.

The speed of a process in long-term investigations may differ considerably, e.g., when it is driven by the ambient climate as in many studies on historical objects. In this case, the rate of image storage should be adjusted dynamically. It must be high enough to obey the sampling theorem and as low as possible to save storage space. Once more, temporal phase unwrapping offers a solution, because it provides an instant fringe count. We have used this to trigger the instant of recording images for an optimum number of fringes over the viewing field [10].

ESPI measurements rely on the local correlation of the speckle fields scattered from the object surface at different instants of time and are impeded severely when the fields decorrelate. There are two main causes for such effects. The speckle field is altered by the overall motion of the object (geometric decorrelation) or it may change due to minute changes in the surface texture by processes like corrosion or condensation of water, to name just two [11]. Either kind of decorrelation will spoil the quality of the measurement and limit the range of applicability.

Often, in-plane motion causes a displacement of the sub-areas that are compared in the correlation. A straight-forward calculation with fixed coordinates suffers from a mismatch because only part of the data within each area contributes to correlation. This is especially pronounced in microscopic ESPI where areas of less than a square millimeter are investigated. We had to develop means to cope with this kind of geometric decorrelation. The Fourier-transform technique of handling spatially phase-shifted data provides an elegant way to do so [12].

Recall that the Fourier-transform method reestablishes the complex object wave. From this we can compute also the intensity distributions for the object states compared that are ordinary speckle images we would get without any reference wave. Now, we can use these images to apply the familiar technique of digital image correlation DIC and obtain the geometrical in-plane mismatch for each correlation sub-area (cf. a following section for more details about this method). The resulting values are used to backshift one of the images for better superposition and then process the ESPI data on optimal matching sub-areas (adaptive windowing).

The improvement in the performance thus obtained is best illustrated by examples from microscopic ESPI. In the investigation of stone deterioration, for example, researchers strive to understand how pressure from the crystallization of salts within the porous stone contributes to the weakening of the material. With pore-sizes of typically less than 100µm deformation measurements request high spatial resolution which can only be obtained under a microscope. For this purpose we have integrated a commercial microscope of long viewing distance into an ESPI setup. Another application is in the study of crack formation in historical paint layers. The famous Chinese terracotta warriors of Lin Tong, for example, loose their invaluable paint cover almost the moment they are excavated, because the originally moist paint layers break up when getting dry. We participate in testing remedies for their conservation.

Fig. 4 was obtained in an ordinary ESPI-study of paint layers on terracotta samples while the humidity was changed – a measuring field of size $230\times230\ \mu m^2$ is inspected. The saw tooth pattern in the left of Fig. 4, obtained in the traditional way, shows useful saw tooth fringes over certain areas, but contains several noisy regions void of fringes because the underlying speckle fields decorrelate. With back-shifting according to the strategy explained above the same data yielded the central pattern of Fig. 4 showing fringes also over most of the area that could not be evaluated before. Obviously, the backshift data also give the in-plane displacement values supplementing the out-of-plane data from ESPI (Fig. 4 right). It is clearly seen how patches in the image that each can be attributed to a flake of paint move individually. A few spurious displacement vectors are measurement errors and could be eliminated by post-processing. Thus, a single ESPI record can now provide the complete 3D displacement field – a task that usually needs three optical configurations of complementing sensitivity vectors. In case of little decorrelation the in-plane component can be obtained with accuracy similar to the out-of-plane component [12].

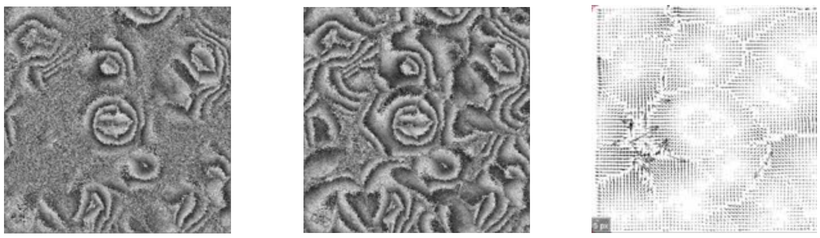

Fig. 4. Elimination of geometric decorrelation in microscopic ESPI by adaptive windowing. Object: painted terracotta (Chinese terracotta army) under the influence of humidity. Left: original saw tooth pattern; center: back-shifted window; right: in-plane deformation.

4. DIGITAL IMAGE CORRELATION

The back shift was determined by digital image correlation DIC. Let us spend a few words on this method because it is an important alternative to ESPI. It allows efficient in-plane mapping of displacements when these are large enough for a non-interferometric method [13]. Two or more ordinary images of the object – either speckle images in laser light or white light photographs – are analyzed for local displacements. For this purpose, the images are subdivided into a matrix of small interrogation regions. Details in the images serve as markers, the smaller they are the better is the sensitivity of the method. White-light photographs can do the job for objects that provide suitable image features. Laser illumination is used in rough-surface objects without sufficient object details, in this case speckles serve as markers. Images are usually recorded electronically and processed with sub-pixel accuracy. Contrary to ESPI, the experimental setup is extremely simple consisting of light source, CCD-camera and computer.

DIC in either version is an established technique and has been applied repeatedly also to tasks in artwork diagnostics. For on-the-site investigations the white-light version provides a robust setup of sensitivity well in the µm-range. We used it, for example, in the monitoring of the response of antique leather tapestry to changes in temperature and humidity. Laser speckle instruments were used in the same project to determine basic data of leather under mechanical and thermal loads [14].

In its primary form, DIC gives only the in-plane displacement values. Since it is a robust technique extremely well suited also for artwork measurements it was investigated how DIC could be turned into a fully 3D-technique. It was shown that an analysis of the shape of the correlation peak or the cross power spectrum of the speckle images under comparison provides the local tilt from which the displacement can be calculated by integration [15]. The accuracy of the out-of-plane displacement thus obtained, however, falls one order of magnitude short of the in-plane component. The technique also allows to distinguish decorrelations due to tilt and microstructure changes.

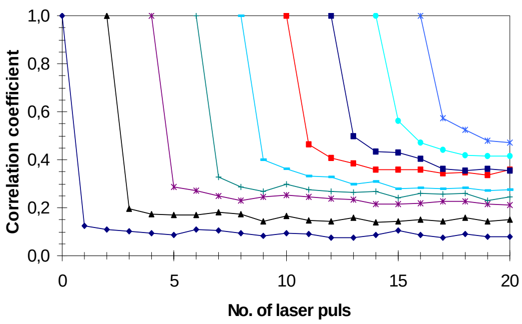

Fig. 5. Monitoring of dirt removal from a historic sandstone sample by speckle correlation. Material is ablated by green Nd:YAG-laser pulses. The family of graphs is obtained by using new reference images in the course of the process.

We mentioned that decorrelation is of disadvantage in displacement mapping. On the other hand, the reduced correlation coefficient can be used as a measure for changes in the topography of a rough surface that reveals, for example, the action of microscopic processes responsible for artwork decay. We have utilized decorrelation analysis for various issues in artwork research [16] – let us show its performance by just one example.

Lasers are often used to clean artwork by ablation of dirt. Efficient monitoring is needed of the ablation process to make sure that only the dirt is removed and no damage is done to the invaluable substance underneath. For this purpose we take speckle images of the surface under treatment for each laser shot and use the decrease in the correlation coefficient to indicate the amount of matter removed. A thorough analysis with varying surface models had to be carried out to quantify the average change in the surface profile causing the decrease in correlation [16]. Fig. 5 presents the set of correlation coefficients versus the number of laser shots in the cleaning of a sandstone sample by green 400-mJ Nd:Yag-laser pulses. The family of graphs is obtained by using new reference images after several shots. Our modeling allowed us to assign an average removal of 70 µm to a decorrelation coefficient of about 0.1. The results show that the first pulse already removes that much; later pulses, however, produce decreasing effects. In suitable object/dirt combinations we expect that the rate of ablation will change markedly when the underlying substance is reached.

5. EXPLORATION OF SAMPLE DEPTH: LOW-COHERENCE SPECKLE INTERFEROMETRY

The optical tools introduced so far make use of light that has been scattered by the specimen and carries mainly information about the location and micro-topography of the surface of a sample. Any conclusions about what is happening in the bulk of the object are indirect. Yet, many practical problems grow underneath the surface of an object and it would be of advantage to have direct access to these regions. As a typical example, take the detachment of paint and varnish layers in the Chinese warriors already mentioned. It is assumed that this stratified heterogeneous compound structure suffers damage because the various layers differ in their mechanical response to the change in ambient humidity. When excavated from the humid soil and moved into dry air, for example, a paint layer may shrink differently from a primary coating or the carrier material. To test such assumptions and provide for countermeasures by conservation agents it would be ideal to map deformations also for various depths in the material.

Light can be used for this purpose if it penetrates deep enough into the material and is sufficiently scattered backwards for detection. When thin paint or varnish layers are involved these are typically only some 100 µm or less in thickness. Often, there is quite a bit of light returning from these depths that can be used for metrological purposes. However, a method is needed to discriminate the light according to the depth from where it has been scattered. This challenge can be met by making proper use of the coherence of light as in optical coherence tomography OCT. We have proposed a combination of OCT with ESPI that we call low-coherence speckle interferometry LCSI [17].

The basic strategy is easily explained. In ESPI, object and reference wave that are obtained by beam-splitting must superimpose coherently to preserve phase information in the CCD-images. Interference of light, however, is only possible when the paths traveled by the waves do not differ by more than the coherence length. Usually, researchers avoid worrying about this requirement by using laser-light sources with a coherence length exceeding all scales involved. On the other hand, low-coherence light – as from a superluminescence diode (SLD) of some 50 µm in coherence length – imposes restrictions on interference experiments. With this light source in combination with a proper design of the optics interference patterns can occur only for signals within an accordingly small path difference and thus identify light from a well defined layer in depth.

Fig. 6 explains the optical setup for LCSI. Light from the SLD is coupled into fibers for reference beam and object illumination. While the reference beam is fed into the ESPI optics as usual, the object light exiting from the fiber is collimated by a lens on a translation stage to illuminate the object. The geometric arrangement in the setup defines a thin "coherence layer" in space such that only light scattered within this region contributes to the interferograms evaluated for displacement. Adjustment of position and orientation of the object allow placing this layer at the desired location within the object. With the translation stage the coherence layer can then be scanned through the sample for investigations at varying depths.

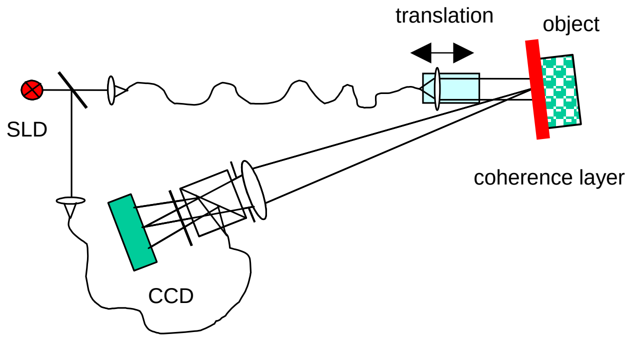

Fig. 6. Optical setup for low coherence speckle interferometry LCSI.

In practice, the useful interference signal has to compete with a large amount of background light. Furthermore, the useful light has to travel through a complex scattering medium that is affected by the changes of the object between the instants of observation. Let us, for example, adjust the coherence layer onto an interface between paint and terracotta in a fragment of a Chinese warrior. We are interested in any motion of the interface during drying. On its way to and from the interface, however, the light has to pass through the bulk of paint – a path that quite probably will be influenced during drying. This produces uncorrelated changes in the light and reduces the quality of the resulting fringes. Therefore, the technique will find its limits at a certain depth that we are exploring presently.

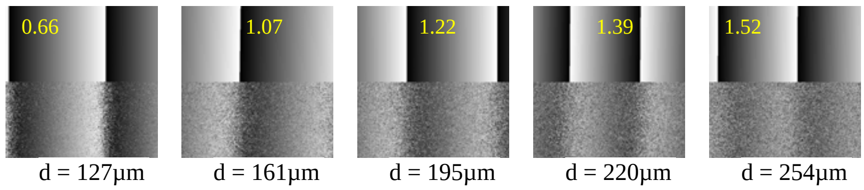

Fig. 7. Performance of LCSI through scattering layers of adhesive (thickness d). Tilt-induced saw tooth fringes for out-of-plane motion of interface between glass carrier and adhesive layer. Lower row: experimental saw tooth; upper row: theoretical fit; numbers: standard deviation σ in rad [18].

For an estimate of the depth range available for exploration a model sample has been studied (Fig. 7) [18]. It was prepared from a partly transparent adhesive (index of refraction n ≈ 2) that is used in bonding and that was coated in steps of varying thickness onto a glass plate. The coherence layer was adjusted to the interface adhesive/glass to observe its out-of-plane motion due to a slight tilt of the specimen. We observe evenly spaced saw tooth fringes that are parallel to the tilt axis and represent the motion introduced. With increasing thickness of the top layer the quality of the fringes decreases due to decorrelation of the underlying speckle signals. By fitting ideal fringe functions (shown above each result) to the experimental data the standard deviation σ of the phase in radians is calculated as a measure for fringe quality [5]. The results for σ indicate the evident loss in fringe quality with increasing thickness, the maximum value is $\sigma = 1.8$ rad and occurs in a random noise pattern, i.e., for complete decorrelation. According to such results one can expect successful measurements for a layer thickness of up to a few 100 µm – subject to the specific properties of the material.
Let us illustrate the potential of LCSI in a first application during out-of-plane measurements on paint layers of the Chinese warriors. Humidity effects were studied in a terracotta fragment that carried a layer of varnish on top of a layer of paint. Thus, in addition to the interface air/varnish at the surface a second reflecting interface was located 70 µm below the surface. By tuning the coherence layer onto either of these interfaces we wanted to measure relative motions between these layers. The left part of Fig. 8 shows the specimen in ordinary illumination, in the bright area at the upper left the top layer is missing and we are looking directly onto the second interface. Deformations were observed due to a change in ambient humidity from 60% to 70%. In the center of Fig. 8 we give the fringe result for the surface, at the right for the lower interface. The surface develops almost a complete deformation fringe while the lower interface has hardly moved at all. This result seems to indicate that humidity is penetrating only slowly to the lower varnish layer.
In summary, LCSI is a promising tool to explore the deformation scene also within a thin region below the surface of rigid objects. The depth available depends on the optical properties of the material – mostly it will not exceed a millimeter. Since action from an aggressive environment, however, has to penetrate a layer immediately adjacent to the surface its mechanical properties become especially important.

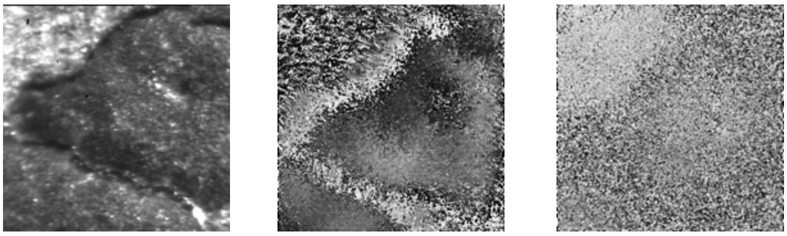

Fig. 8. Humidity-induced motion of the surface and an interface at 70 µm in a layered coating on a Chinese terracotta sample. Relative humidity changed from 60% to 70%. Left: view of sample; center: saw tooth fringes from surface; right: saw tooth fringes from interface.

6. SOUNDING THE DEPTH – VIBRATION ESPI

Many historical murals are carried by plaster layers of up to several centimeters in thickness. In the course of time, such layers may detach from the supporting wall – thus a check of the integrity of the interface is needed. We have shown that low-coherence exploration of an object below its surface is possible, but restricted to rather short depths. Thus, light can not be used directly to scan the depth for detachments and we must develop other means. We can use the light, however, to probe the minute response of loose areas to an acoustic-wave stimulus “sounding” the depth for an optical alert signal.

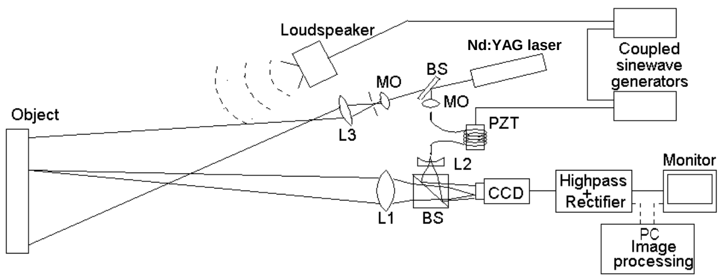

Fig. 9. Time average ESPI-system for the study of detached layers in murals. Loudspeaker sound excites the layer. Reference-beam modulation at a slightly offset frequency shifts the working point to maximum sensitivity, provides for phase shifting and results in flickering light in vibrating areas.

ESPI is a perfect tool in studying small vibrations [19] that we adapted to the mural problem. In our setup (Fig. 9) an ordinary time average ESPI arrangement is refined by modulation of the reference-beam phase with a frequency slightly displaced from the loudspeaker signal. This has several advantages. Firstly, we can move the operating point in the fringe function to the place of maximum sensitivity. Secondly, the beat between reference and signal waves produces flickering light intensities at those locations that take part in the vibration. This is a very intriguing feature because it implies intuitively the state of “motion” – an argument important when advertising a high-tech method to the community of restorers and conservators. Finally, several images captured during a beat cycle provide the basis for temporal phase shifting to yield automated evaluation of vibration amplitude and phase. The final equipment is characterized by a fiber optic reference link which provides the basis for phase modulation (PZT-driven fiber manipulation) and even allows path length matching by introducing additional fiber length. The coherence constraints, however, are low since we changed from our early laser-diode illumination to a very stable CW Nd:YAG laser. Performance is improved by robust setups and averaging over several images which allows to do on-the-site measurements of vibration amplitudes of as little as a few nm.

The measurement strategy in mural investigations is to look for resonances while tuning the excitation through an appropriate frequency band. For Fig. 10 the technique was tested at an artificially produced detached area in a stone wall. We show phase and amplitude maps of a 230-Hz resonance mode in the plaster layer. Many such results obtained at 10-Hz frequency steps from 90 Hz to 580 Hz were finally accumulated to produce the map at the right of Fig. 9. Color indicates how often a certain location had responded to the excitation – red areas vibrated often, green ones rarely. The location and shape of the loose region are nicely reproduced.

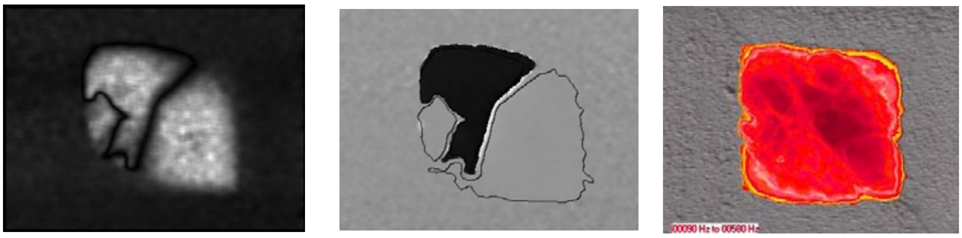

Fig. 10. 230-Hz vibration of an artificially produced detachment in a plaster layer on a stone wall. Left: amplitude map of higher-order mode of the cover plate; center: phase map; right: final evaluation of excitation response between 90 Hz and 580 Hz in 10 Hz-steps indicating the loose area.

Additional information from the vibration data can be utilized for depth sounding. Thick layers respond at low, thin layers at higher frequencies. In a multi-layer plaster this allows speculations about the depth of the damaged interface. For an example, we present results of a study on a two-layer plaster coating at a historical wall that was checked for the success of a remedy in which restorers injected a fixing cement through a certain number of small holes. Studies at a location where the upper layer was missing revealed that the lower layer responded mostly to frequencies below some 800 Hz. Thus, we grouped our results into two maps, one considering all data below, the other above 800 Hz. Blue and red hatched areas in Fig. 11 indicate all positive responses for the low and high frequency range, respectively; the width of the scene was 0.9 m. The results clearly show that the lower interface was not repaired as we find one large vibrating region in the low-frequency domain that includes the location of most of the fixation points. The response of the thinner upper layer (indicated by the many small regions in the high-frequency map) respects most of these points. Probably, the holes did not penetrate through the second layer and the cement connected only the two layers, but did not attach them to the wall.

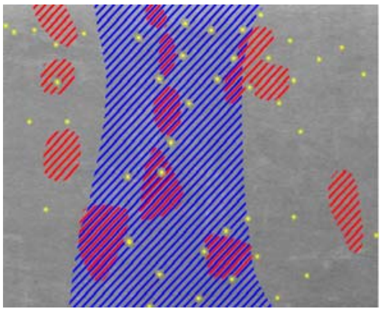

Fig. 11. Localization of detachments in a two-layer plaster on a wall in the *Neues Museum*, Berlin. Results of a series of ESPI measurements at equidistant frequencies. The hatched areas indicate regions where the lower interface (blue, response to frequencies below 800 Hz) or the upper interface (red, frequencies above 800 Hz) are considered loose. The yellow dots indicate cement injections.

Meanwhile, the method has found application in renowned places investigating large areas that would otherwise require elaborate efforts. An advantage over the traditional method of manual testing is its objectiveness which is important when progressing detachments are to be revealed. Mechanical modeling of vibrating layers may assist in drawing even more information about the state of the object from the vibration data.

7. CONCLUSIONS

Techniques of coherent optical metrology have proven well-suited for the investigation of the mechanical processes involved in the deterioration of artwork. They offer the necessary sensitivity to explore displacement fields and surface changes, and they are non-invasive which is of essential importance in delicate historical pieces. While the basic usefulness has been shown in various problems the metrology must now be developed for general acceptance as a tool in the everyday tasks of restorers and conservators.

ACKNOWLEDGEMENT

This presentation is a summary of work that has mainly been carried out in the Applied Optics Group at the Institute of Physics in Oldenburg. The dedicated contributions of many former members of the group enter into our results which we acknowledge gratefully. Special mention deserves the doctoral thesis work of J. Burke and T. Fricke-Begemann, who have contributed essentially to our progress in speckle metrology. Recent advances in LCSI are benefiting from a cooperation with K. Gastinger at SINTEF, Trondheim, Norway. We also acknowledge the financial support from DFG, BMBF and DBU in Germany.

BIBLIOGRAPHY

[1] D. Paoletti and G.S. Spagnolo: Interferometric methods for artwork diagnostics. *Progress in Optics* XXXV, 167. Elsevier, Amsterdam (1996).

[2] K. Hinsch and G. Gülker: Lasers in art conservation. *Physics World* **14** , 37-42 (2001).

[3] G. Gülker, H. Helmers, K.D. Hinsch, P. Meinlschmidt, K. Wolff: Deformation mapping and surface inspection of historical monuments. *Opt. Las. Eng.* **24**, 183-213 (1996).

[4] K. Creath: Phase-shifting speckle interferometry, *Appl. Opt*. **24**, 3053-3058 (1985).

[5] Burke, Jan; Universität Oldenburg, FB Physik, AG AOP: *Application and optimization of the spatial phase shifting technique in digital speckle interferometry*. Dissertation University of Oldenburg, (2000). Document at http://www.physik.uni-oldenburg.de/Docs/holo/paper/Dissertation_Jan_Burke_2000.pdf)

[6] T. Bothe, J. Burke, H. Helmers: Spatial phase shifting in electronic speckle pattern interferometry: minimization of phase reconstruction errors. *Appl. Opt.* **35**, 5310-5316 (1997).

[7] M. Takeda, H. Ina, S. Kobayashi: Fourier-transform method of fringe-pattern analysis for computer-based topography and interferometry. *J. Opt. Soc. Am*. **72**, 156-160 (1982).

[8] J. Burke, H. Helmers, C. Kunze, V. Wilkens: Speckle intensity and phase gradients: influence on fringe quality in spatial phase shifting ESPI-systems. *Optics Comm.* **152**, 144-152 (1998).

[9] J. Huntley, H. Saldner: Temporal phase-unwrapping algorithm for automated interferogram analysis. *Appl. Opt.* **32**, 3047-3052 (1993).

[10] J. Burke and H. Helmers: Matched data storage in ESPI by combination of spatial phase shifting with temporal phase unwrapping. *Opt. Las. Technol*. **32**, 235-240 (2000).
[11] G. Gülker, K.D. Hinsch: "Detection of surface microstructure changes by electronic speckle pattern interferometry", *J. Opt. Las. Eng*. **26**, 165-178 (1997).
[12] T. Fricke-Begemann and J. Burke: Speckle interferometry: three-dimensional deformation field measurement with a single interferogram. *Appl. Opt*. **40**, 5011-5022 (2001).
[13] M. Sjödahl: Digital speckle photography. In: *Digital Speckle Pattern Interferometry and Related Techniques* (ed. P.K. Rastogi), Wiley, Chichester (2001).
[14] K. D. Hinsch, G. Gülker, H. Hinrichs, H. Joost: Artwork monitoring by digital image correlation. In: *Lasers in the Conservation of Artworks* (ed. K. Dickmann, C. Fotakis, J.F. Asmus). LACONA V Proceedings, Springer-Verlag, Berlin (publication Sept. 2004).
[15] T. Fricke-Begemann: Three-dimensional deformation field measurement with digital speckle correlation. *Appl. Opt.* **42**, 6783-6796 (2003).
[16] T. Fricke-Begemann, K. D. Hinsch: Measurement of random processes at rough surfaces with digital speckle correlation. *J. Opt. Soc. Am*. **A 21**, 252-262 (2004).
[17] G. Gülker, K.D. Hinsch, A. Kraft: Deformation monitoring on ancient terracotta warriors by microscopic TV-holography. *Opt. Las. Eng*. **36**, 501-513 (2001).
[18] K. Gastinger, G. Gülker, K.D. Hinsch, H.M. Pedersen, T. Støren, S. Winther: Low coherence speckle interferometry (LCSI) for detection of interfacial instabilities in adhesive bonded joints. In: *Interferometry XII* (ed. W.Osten, E. Novak), SPIE Proc. **5532**, paper 26 (2004).
[19] S. Ellingsrud, G.O. Rosvold: Analysis of a data-based TV-holography system used to measure small vibration amplitudes. *J. Opt. Soc. Am.* **A9**, 237-251 (1992).